Deep–Sea Research I 179 (2022) 103668

Contents lists available at ScienceDirect

Deep-Sea Research Part I

journal homepage: www.elsevier.com/locate/dsri

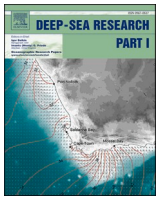

Research Paper

Microbial communities associated with sinking particles across an environmental gradient from coastal upwelling to the oligotrophic ocean

Bellineth Valencia [a,*], Michael R. Stukel [b], Andrew E. Allen [a,c], John P. McCrow [c], Ariel Rabines [c], Michael R. Landry [a]

[a] Scripps Institution of Oceanography, University of California San Diego, La Jolla, CA, USA
[b] Earth, Ocean, And Atmospheric Science Department, Florida State University, Tallahassee, FL, USA
[c] Microbial and Environmental Genomics, J Craig Venter Institute, La Jolla, CA, USA

ARTICLE INFO

Keywords:
Biological carbon pump
Particle-attached microbes
Phytoplankton
Bacteria
Protists
Bacillariophyceae

ABSTRACT

Complex interactions between microbial communities in the epipelagic and mesopelagic ocean drive variability in sinking carbon flux as part of the biological carbon pump. To investigate the relative contribution of dominant prokaryotic, protistan, and phytoplankton taxa to sinking particles, we used 16S/18S rRNA gene sequencing of particles collected in sediment traps and water column communities. Comparisons were done across a coastal upwelling-to-oligotrophic environmental gradient in the southern California Current Ecosystem to assess effects of natural environmental variability on taxon-specific contributions to sinking particle export. Particle-associated microbial assemblages differ from ambient mixed-layer communities. Gammaproteobacteria, dinoflagellates, and rhizarians were dominant microbes associated with sinking particles at all sampling locations, with diatoms increasing significantly at the inshore mesotrophic site. Parasitic groups, syndiniales and apicomplexans, were also major particle-associated taxa. Relative sequence abundance on exported particles from the mesotrophic inshore site more closely resembled the water-column dominants (especially diatoms) found above, while oligotrophic communities exhibited greater dissimilarity between the microbial communities on sinking particles and in the mixed layer. Protists generally showed greater similarity between mixed-layer and sinking particle communities than prokaryotes. *Synechococcus* was over-represented on sinking particles (relative to eukaryotic phytoplankton and other cyanobacteria) only in oligotrophic areas. Diatoms were the only phytoplankton group consistently over-represented on sinking particles across the region. Our results highlight important variability in microbial contributions to export that seem to align with differences in dominant grazing pathways. At the upwelling influenced site where export was primarily due to the fecal pellets of large copepods, diatoms were dominant contributors to export and protistan communities on sinking particles resembled those in the water column above. When doliolids were abundant, dinoflagellates contributed substantially to export, while the dominant picoeukaryote (*Ostreococcus*) was only a minor contributor. In oligotrophic areas, where grazing pathways were dominated by protists and sinking particles were primarily amorphous aged aggregates, there was little similarity between mixed layer and sinking particle communities.

1. Introduction

Predicting changes in marine carbon sequestration requires a detailed understanding of the ocean's biological pump (BP) that transports organic carbon fixed by phytoplankton into the deep ocean (Buesseler and Boyd, 2009; Ducklow et al., 2001; Martin et al., 1987). The BP transforms organic particles physically and chemically through multiple food-web pathways and processes spanning all domains of life and spatiotemporal scales (Burd et al., 2016; Frischknecht et al., 2018). Export and sequestration efficiency are shaped not only by surface primary production, but also by particle sinking speeds and remineralization rates (Cram et al., 2018; McDonnell et al., 2015), the microbial ecology of sinking particles (Pelve et al., 2017; Piontek et al., 2009), and flux-feeding taxa in the mesopelagic (Jackson et al., 1993; Stukel et al.,

Abbreviations: BP, biological pump; CC, California Current Proper region; IN, Inshore region; OO, Oligotrophic offshore region; OTU, operational taxonomic unit; SSU-rRNA, small subunit ribosomal RNA gene; TZ, Transition zone region; WC, water column.

* Corresponding author.
E-mail address: bellival@ucsd.edu (B. Valencia).

https://doi.org/10.1016/j.dsr.2021.103668
Received 15 July 2021; Received in revised form 14 October 2021; Accepted 5 November 2021
Available online 12 November 2021
0967-0637/

2019b). These interacting processes, with varying importance in different regions and seasons, complicate simple predictions of export flux from primary production and necessitate integrative studies that link ecology and biogeochemistry (Burd et al., 2016; Siegel et al., 2016).

Advances in genetic characterization of communities, especially when combined with existing sediment trap methodologies, have recently allowed new investigations of microbial communities that create, modify, colonize, and remineralize sinking particles. These studies have shown, for instance, that *Synechococcus* is overrepresented on sinking particles relative to *Prochlorococcus* (Amacher et al., 2013) and uncovered an unexpectedly large role for Rhizaria in sinking flux (Guidi et al., 2016; Gutierrez-Rodriguez et al., 2019). They have also provided evidence of significant community shifts on sinking particles (Fontanez et al., 2015; Gutierrez-Rodriguez et al., 2019; Pelve et al., 2017) and vertical connectivity between the euphotic zone and bathypelagic realm (Mestre et al., 2018; Ruiz-González et al., 2020). Time-series studies at abyssal depths have further documented relatively consistent dominance by piezophilic groups, variable contributions of eukaryotic taxa (Boeuf et al., 2019), and even major episodic flux events attributed to single diatom species (Preston et al., 2019). To date, however, most such studies have focused on a single ecological condition (e.g., the Sargasso Sea. Amacher et al., 2013) or have not quantified sinking particles and attached microbes (e.g., Guidi et al., 2016; Mestre et al., 2018).

In the present study, we investigate spatial patterns in suspended and sinking eukaryotic and prokaryotic communities in the California Current Ecosystem (CCE). The CCE is an excellent natural laboratory for such studies, because it includes an environmental gradient ranging from coastal upwelling to the edge of the oligotrophic North Pacific Subtropical Gyre within a compact spatial region (Ohman et al., 2013; Stukel and Barbeau, 2020). The coastal upwelling zone is characterized by high biomass and dominance of larger primary producers (Venrick, 2002; Taylor et al., 2015), and exported particles are mostly composed of zooplankton fecal pellets (Knauer et al., 1979; Stukel et al., 2013; Morrow et al., 2018). In contrast, the offshore open-ocean region has low biomass and dominance of small cells (Taylor and Landry, 2018), and exported particles are mainly amorphous aggregates (Knauer et al., 1979; Stukel et al., 2013; Morrow et al., 2018). Using Lagrangian drifters to follow marked water parcels on process cruise P1604 (April–May 2016) of the CCE Long-Term Ecological Research (CCE LTER) Program, we combine traditional biogeochemical rate and standing stock measurements with 16S and 18S rRNA gene sequencing of microbial communities for particles collected in sediment traps and sampled from the mixed layer, base of the euphotic zone, and 150 m. We focus on two hypotheses: 1) sinking material more closely reflects the water-column dominants in productive coastal waters than offshore oligotrophic waters due to larger taxa (e.g., diatoms, larger mesozooplankton), shallower euphotic depth, and more rapid, direct sinking of POM in coastal waters; and 2) the composition of eukaryotic taxa is more similar between water-column and sinking particles than prokaryotic taxa because the larger eukaryotes are more likely to sink rapidly as aggregates or in zooplankton fecal pellets.

2. Methods

2.1. Sample collection and environmental measurements

Data are derived from the P1604 Process cruise of the CCE LTER Program (19 Apr - 12 May 2016; Kelly et al., 2018; Nickels and Ohman, 2018). The cruise took place during the end of the 2015–2016 El Niño, which followed the North Pacific marine heat wave of 2014–2015 (Bond et al., 2015; Jacox et al., 2016; Kahru et al., 2018). The region had thus experienced exceedingly warm conditions with reduced upwelling for some time, although upwelling resumed near the coast during our cruise. The cruise sampling plan featured four Lagrangian experiments of ~3 – 5-day duration, during which two drifting arrays with 3 × 1-m drogues were used to track mixed-layer communities (Landry et al., 2009). One array held sediment traps (see below), while the other contained attachment points for daily in situ incubations conducted to measure primary productivity using $H^{14}CO_3^-$ uptake (6 depths per day), among other measurements (see Morrow et al., 2018). Daily CTD casts were conducted at 02:00 (to collect water for daily incubations and standing stock measurements at 6 depths in the euphotic zone) and at approximately local noon (to determine photosynthetically active radiation profiles). Nutrients were measured using an autoanalyzer. Chlorophyll (Chl) *a* (total and size-fractionated) was measured using the acidification method. Heterotrophic bacteria, *Prochlorococcus, Synechococcus,* and picoeukaryotes were enumerated by flow cytometry. Mesozooplankton biomass and community composition was determined from paired day-night 202-μm mesh bongo net samples (Morrow et al., 2018; Nickels and Ohman, 2018). Samples for DNA analyses were collected from Niskin bottles at the mixed layer, the base of the euphotic zone, and 150 m (Table S1). Seawater samples (280 mL, 200 μm Nitex screen or 650 mL, 500 μm Nitex screen) were filtered onto 0.2-μm Supor membrane filters (Pall), flash-frozen, and stored at −80°C until analysis.

VERTEX-style cylindrical sediment traps (12 tubes per depth) were deployed on the trap array at fixed depths of 100 and 150 m, with additional traps placed at the base of the euphotic zone at the two sites closest to shore (Knauer et al., 1979; Morrow et al., 2018). Traps with top baffles were deployed with a formaldehyde brine (filtered seawater + 50 g L^{-1} NaCl + formaldehyde (0.4% final concentration); for most analyses), an unpoisoned brine (for sequencing), or RNA later (also for sequencing, prepared following methods in Fontanez et al., 2015). Independent ^{238}U–^{234}Th deficiency measurements confirmed that the traps had no consistent over- or under-collection bias (Stukel et al., 2019a). After recovery, all tubes were filtered through a 200-μm filter, which was then carefully inspected by stereomicroscope and mesozooplankton 'swimmers' were removed, before the remainder of the >200-μm material were frozen at −80ºC. Tubes were then split and filtered for analyses including POC and PN, Chl *a*, phaeopigments, fecal pellet mass flux, ^{234}Th, and sequencing. Samples from the unpreserved (live) and RNA later traps were immediately filtered through Sterivex filters (Millipore, 0.22 μm) and frozen at −80°C for 18S/16S rRNA gene sequencing analyses. Samples for POC and PN were filtered through pre-combusted GF/F filters, frozen, acidified on land, and analyzed by an elemental analyzer coupled to an isotope ratio mass spectrometer. Samples for Chl *a* and phaeopigments were filtered through GF/F filters and analyzed by the acidification method. Samples for fecal pellet mass flux were analyzed using a stereomicroscope (20X magnification). Fecal pellets were categorized by shape and morphometric measurements were determined by image analysis and qualitative characteristics of sinking material (e.g., dominance by fecal pellets or aggregates) were noted. Samples for ^{234}Th were filtered through QMA filters and analyzed using a RISO low-level beta multi-counter. For additional details on other analyses and general sediment trap processing, see Morrow et al. (2018) and Stukel et al. (2019a).

The Lagrangian experiments sampled four regions of differing trophic conditions in the CCE: 1) offshore oligotrophic (OO) waters on the edge of the subtropical gyre, 2) core water of the California Current (CC), 3) the transition zone (TZ) region where inshore mesotrophic waters were mixing with the edge of the California Current, and 4) inshore (IN) nutrient-rich water showing evidence of recent upwelling. Additional environmental data from these experiments are available on the CCE LTER Datazoo website.

2.2. Library construction and sequencing

DNA from water-column and trap samples was extracted using the NucleoMag 96 Plant kit (Macherey Nagel) following the manufacturer's instructions. Although DNA was extracted separately for the sediment trap particles <200 μm and >200 μm, these were pooled for subsequent analysis. DNA was amplified by Polymerase Chain Reaction using the Q5

high-fidelity PCR kit (New England Biolabs). Prokaryotes were characterized by amplification of the V4–V5 regions of the 16S small subunit ribosomal RNA gene (SSU-rRNA) using primers 515F and 926R (Quince et al., 2011) (Table S2). Eukaryotes were characterized by amplifying the V9 region of the18S rRNA gene using primers 1389F and 1510R (Amaral-Zettler et al., 2009) (Table S2). For sediment trap samples that did not amplify during PCR, we used the OneStep™ PCR Inhibitor Removal Kit (Zymo Research) to remove inhibitory substances.

The PCR products were pooled in equimolar amounts (~10 ng μL^{-1}) and sequenced using a dual-barcode index on an Illumina MiSeq platform at the Institute for Genomic Medicine (IGM, University of California, San Diego). Initial quality control of the raw sequence reads was done using the workflow for read filtering, swarm Operational Taxonomic Unit (OTU) clustering, and taxonomic classification of the SSU-rRNA written by JP McCrow (https://github.com/allenlab/rRNA_pipeline). Demultiplexed raw reads were provided by IGM and have been deposited in NCBI under BioProject PRJNA445287 and Biosample accession numbers SAMN08784582–SAMN08784552 for 18SrRNA gene sequences, and under BioProject PRJNA422420 and Biosample accession numbers SAMN08784494–SAMN08784464 for 16S rRNA gene sequences. Additional processing details are in the Supplementary Information. The total number of sequence reads and OTUs are summarized for each primer set in Table S3 and by sample types in Table S4 (prokaryotes) and Table S5 (eukaryotes). These results show relative contributions of different taxa in each sample, but should not be interpreted as differences in absolute abundance of taxa across samples (Gong and Marchetti, 2019; Vandeputte et al., 2017). Indeed, the abundance of heterotrophic bacteria at the surface (determined by flow cytometry), varied from 3.2×10^5 cells mL^{-1} at the OO site to 4.8×10^6 cells mL^{-1} at the IN site, while surface Chl *a* (proxy for phytoplankton biomass) varied by a factor of 40.

2.3. Statistical analyses

We evaluated differences in prokaryotic (16S) and eukaryotic (18S) assemblages at the genus level by multivariate analyses based on the Bray-Curtis dissimilarity index. Prior to analyses, the sequence reads were merged by genera (prokaryotes: 379, eukaryotes: 510), and only those contributing >1% to the relative abundances in any sample (prokaryotes: 79, eukaryotes: 97) were included in the analyses. For the genera selected, relative abundances per sample were recalculated and square-root transformed to reduce the impact of the most abundant microbes. Community differences were assessed by hierarchical clustering and ordination using non-metric multidimensional scaling (nMDS). Cluster significance was established by similarity profile analysis (SIMPROF). Multivariate analyses were done in R using the packages 'vegan' (Oksanen et al., 2017) and 'clustsig' (Whitaker and Christman, 2014).

3. Results

3.1. Environmental conditions and export fluxes

Our drifter experiments covered a seven-fold range in productivity (229–1659 mg C m^{-2} d^{-1}) and a six-fold range in sediment-trap carbon fluxes at 150 m (32–202 mg C m^{-2} d^{-1}) (Table 1, Figs. 1 and 2). Environmental conditions in offshore oligotrophic (OO) and California Current waters (CC) were marked by deep mixed layers (50–80 m), low nutrients (0.02–0.08 μM nitrate), low chlorophyll (0.1–0.2 μg Chl *a* L^{-1}), and low primary production (PP, 229–276 mg C m^{-2} d^{-1}) (Table 1, Fig. 1b–d, Fig. 2a–b). In contrast, conditions in the transition zone (TZ) and inshore (IN) areas had shallower mixed layers (30 and 12 m, respectively) with elevated nutrients, Chl *a*, and PP compared to the offshore region. Mixed-layer nitrate concentrations were highest in the TZ region (4.6 vs 2.1 μM), but Chl *a* and PP were greatest at the IN site (4.2 vs 1.2 μg L^{-1} and 1659 vs 868 mg C m^{-2} d^{-1}, respectively). There was also a shift towards larger cells in the upwelling region. The <1-μm size fraction accounted for 59% of chlorophyll at the OO site, while the median (chlorophyll-weighted) cell size was between 3 and 8 μm at the IN site. The transition from offshore (OO) to coastal (IN) regions was also associated with order-of-magnitude increases in mesozooplankton community biomass and grazing (Morrow et al., 2018; Nickels and Ohman, 2018). Mesozooplankton communities were typically dominated by crustaceans (especially copepods), except for a high biomass of doliolids (pelagic tunicates) in the TZ region.

Table 1
Summary of environmental data during sediment trap drift deployments across a gradient of ecosystem conditions in the California Current Ecosystem. PP: primary production (mg C m^{-2} d^{-1}), POC flux: export of particulate organic carbon (mg C m^{-2} d^{-1}), Temperature (°C), Chl: chlorophyll *a* (μg l^{-1}), NO_3: nitrate (μg l^{-1}). Number of chlorophyll-nitrate measurements per depth and CTD casts were as follow: OO (n: 3, 4), CC (n: 7, 10), TZ (n: 6, 11), and IN (n: 7, 11). Mean ± standard error.

Inshore (IN)					
PP	Depth (m)	POC flux	Temperature	Chl	NO3
1658.7 ± 195.6	0–5	–	14.42 ± 0.05	4.20 ± 0.24	1.13 ± 0.15
	47	251.0 ± 8.3	10.39 ± 0.04	0.42 ± 0.06	24.27 ± 2.07
	147	202.3 ± 14.0	8.82 ± 0.04	–	–
Transition Zone (TZ)					
PP	Depth (m)	POC flux	Temperature	Chl	NO3
868.0 ± 133.8	0–5	–	13.63 ± 0.05	1.01 ± 0.03	3.45 ± 0.28
	57	120.4 ± 9.7	11.24 ± 0.06	0.25 ± 0.06	13.21 ± 0.71
	147	77.4 ± 4.4	8.78 ± 0.01	–	–
California Current (CC)					
PP	Depth (m)	POC flux	Temperature	Chl	NO3
275.7 ± 41.1	0–5	–	15.20 ± 0.02	0.13 ± 0.01	0.07 ± 0.04
	97	40.2 ± 3.8	13.18 ± 0.08	0.34 ± 0.06	4.94 ± 1.67
	147	37.0 ± 5.0	9.54 ± 0.03	–	–
Oligotrophic Offshore (OO)					
PP	Depth (m)	POC flux	Temperature	Chl	NO3
229.0	0–5	–	17.26 ± 0.12	0.07 ± 0.00	0.03 ± 0.02
	100	72.1 ± 7.3	12.22 ± 0.05	0.16 ± 0.05	11.16 ± 1.68
	150	31.8 ± 4.9	9.51 ± 0.01	-	-

The composition of sinking particles collected in sediment traps also shifted across the productivity gradient (Fig. 2c–g). In the upwelling region, export was dominated by recognizable mesozooplankton fecal pellets, primarily cylindrical pellets believed to be crustacean egesta. Recognizable pellets contributed nearly all of the carbon flux at the IN site and approximately 50% in the TZ area (Fig. 2d and f). In contrast, recognizable pellets were a negligible component of sinking material in most traps in the offshore region, where most of the carbon was unrecognizable detrital material and aggregates. IN and TZ traps also had substantially higher pigment:carbon ratios than OO or CC traps, reflecting rapid export of pigmented material from the euphotic zone (Fig. 2e). The pigments were predominantly phaeopigments (degradation products of Chl *a* formed during digestion in mesozooplankton guts), suggesting that phytoplankton were consumed by grazers prior to export (Fig. 2g). These ecological and biogeochemical differences are typical of the gradient in ecosystem characteristics across the CCE and underlie the >6-fold difference in POC export fluxes into the 150-m

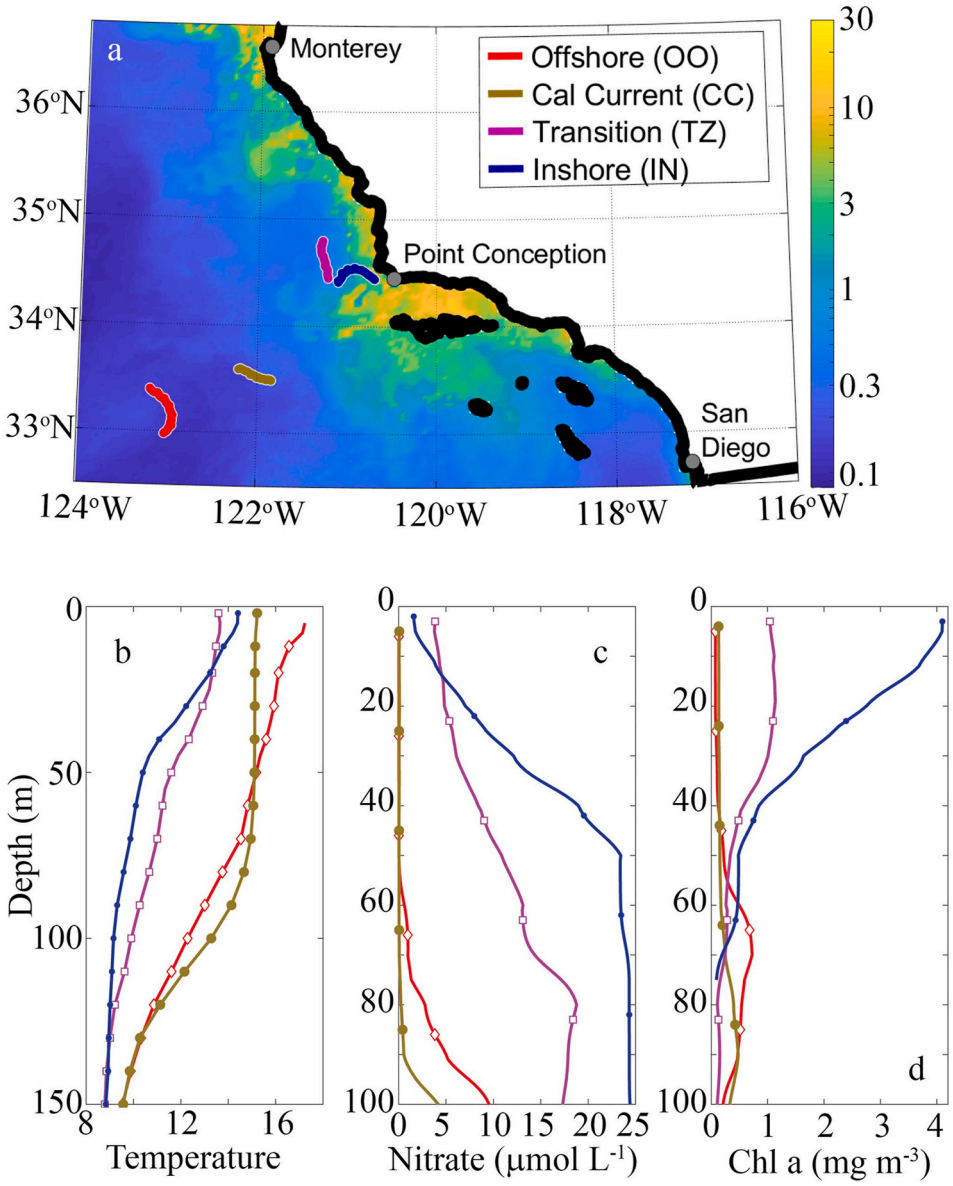

Fig. 1. Map of study region with satellite-derived sea surface Chl (Kahru et al., 2015) and sediment trap drift tracks (a) for OO site (red), CC site (brown), TZ site (magenta), and IN site (blue). Associated vertical profiles (averaged across the Lagrangian experiment) of temperature (b), nitrate (c), and Chl a (d).

traps deployed at the OO and IN sites (Table 1).

3.2. Major groups from sequence analyses: Eukaryotes

We collected water-column samples from multiple depths (typically mixed layer, base of the euphotic zone, and 150 m) and analyzed them for 18S and 16S rRNA gene sequences (Fig. 3). In addition to the protistan reads determined from 18S, we identified numerous metazoan sequences (Fig. 3). Within our working OTU table, which excludes singletons and merges sequence reads of over-split OTUs, metazoans accounted for 1%–63% of total reads, with an arithmetic mean of 27% across all depths and sites. Most of the metazoan sequences are ascribed to copepods, especially the calanoids *Metridia* and *Calanus* spp., both important consumers and vertical migrators in CCE waters (Supp. Fig. 1). Doliolid sequences are also present due to a bloom of *Doliolum denticulatum* during the study period, with highest densities in the TZ. Percent metazoan reads typically increased with depth, except at the TZ site, which had high doliolid abundances in the mixed layer. In contrast to the water column, metazoan sequences were more abundant than protistan sequences (84%–16%) in the sediment traps (mean: 82%), despite the fact that all recognizable >200-μm mesozooplankton "swimmers" were removed from those samples during examination under a stereomicroscope (Fig. 3).

Protist communities in mixed-layer samples are co-dominated by alveolates and stramenopiles at the IN site, chlorophytes (Archaeplastida) are more important in the TZ, and alveolates dominate the OO and CC sites (Fig. 4). Clear shifts were also evident with depth. At the IN and TZ sites, the contributions of stramenopiles and Archaeplastida, respectively, decreased consistently with depth (Fig. 4). In contrast, Rhizaria increased in proportional abundance at deeper depths at all sites. They accounted for ~30% of sequences at 150 m at the IN station and approximately half of the sequences at the other three sites (Fig. 4).

Protistan communities on sinking particles collected by sediment traps were typically dominated by parasitic alveolates (apicomplexan and syndiniales) and rhizarians, although their contributions varied among sampling locations (Figs. 4 and 5). In the IN traps, alveolates and stramenopiles are all important (Fig. 4). At the TZ site, the large contribution of chlorophytes (Archaeplastida) to the water-column

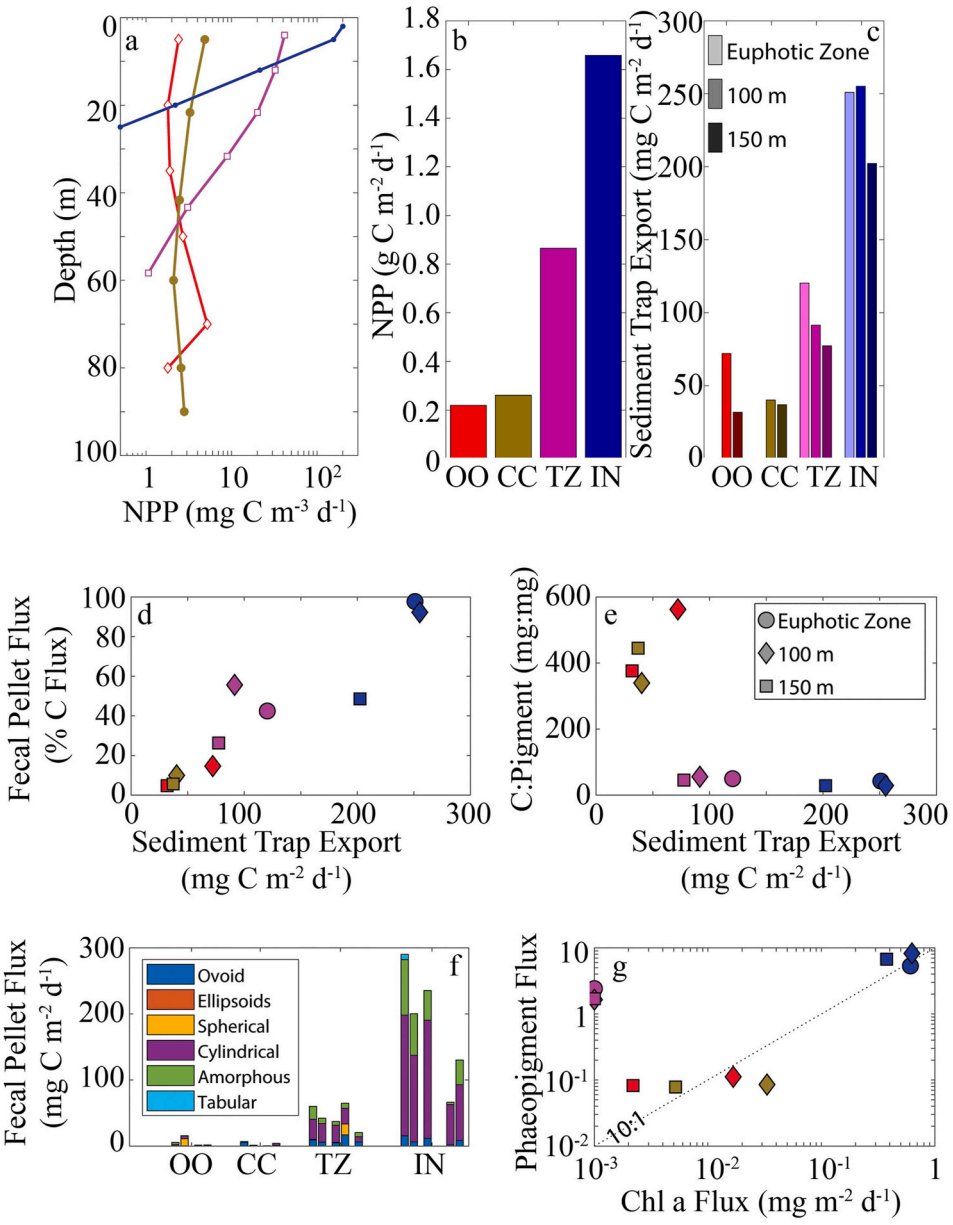

Fig. 2. Net primary production and sediment trap export across the environmental gradient. Vertical profiles (averaged across the Lagrangian experiment) of net primary production (a). Vertically-integrated net primary production (b) and vertical export at three depths (c). Property-property plots show the percentage of carbon flux attributed to recognizable fecal pellets (d) and the carbon to pigment (Chl a + Phaeopigments) ratio of sinking material (e) both as a function of total export and phaeopigment flux plotted against Chl a flux (g). The relative contributions of different fecal pellet types to sinking material at each site is shown in panel (f). In panels a–e and g, colors indicate the sampling location as follows: OO site (red), CC site (brown), TZ site (magenta), and IN site (blue).

assemblage is not seen in the trap samples. In the CC traps, alveolate sequences dominate (except for rhizarians in one live trap), while both alveolates and rhizarians are important in the OO trap samples (Fig. 4).

3.3. Water-column community composition: Eukaryotes

18S rRNA gene sequences from the mixed layer showed substantial variability in protistan communities across the environmental gradient (Fig. 5, Table S6). At the coastal upwelling-influenced IN site, stramenopiles (especially the diatoms *Thalassiosira* and another unclassified Bacillariophyceae) were particularly important, while the chlorophyte *Micromonas* was another important contributor (Fig. 5). TZ samples were characterized by very high abundances of Archaeplastida sequences, including the chlorophyte *Ostreococcus*, which was responsible for 44% of protistan reads. At both of the offshore sites (CC and OO), the protistan community was dominated by alveolates, with high sequence abundances of an uncultured dinoflagellate (16% of reads at OO; 18% at CC). The dinoflagellate *Glenodiniopsis* contributed 28% of mixed-layer sequences at OO, and a third dinoflagellate, *Karlodinium*, was common across the region (from IN to OO) and at multiple depths from the euphotic zone to 150 m. Besides alveolates, the Acantharian Chaunacanthida was particularly important at 150 m, comprising 26%, 55%, and 32% of total protistan reads at the IN, TZ, and OO sites, respectively (Fig. 5). At all sites, multiple groups of marine alveolates (including cultured and uncultured dinoflagellates as well as MALV-I, MALV-II, and MALV-III) comprised most of the remaining sequences.

We used non-metric multidimensional scaling (nMDS, Fig. 5a) and dendrogram (Fig. 5b) analyses based on the Bray-Curtis dissimilarity index, with broadly similar results, to compare assemblage differences across sites, depths, and sampling type (water column or sediment trap). For water-column samples, microbial community structure clusters mainly by depth, although mixed-layer assemblages also differ among locations (Fig. 5). The 150-m samples from all sites are characterized by high concentrations of acantharians and polycystine radiolarians (Fig. 5b, Table S6). Samples from the euphotic zone base in the TZ, CC, and OO regions cluster in a single group that is closely aligned with mixed-layer samples from the CC and OO sites. Euphotic zone samples (both mixed layer and euphotic zone base) from the IN site cluster more

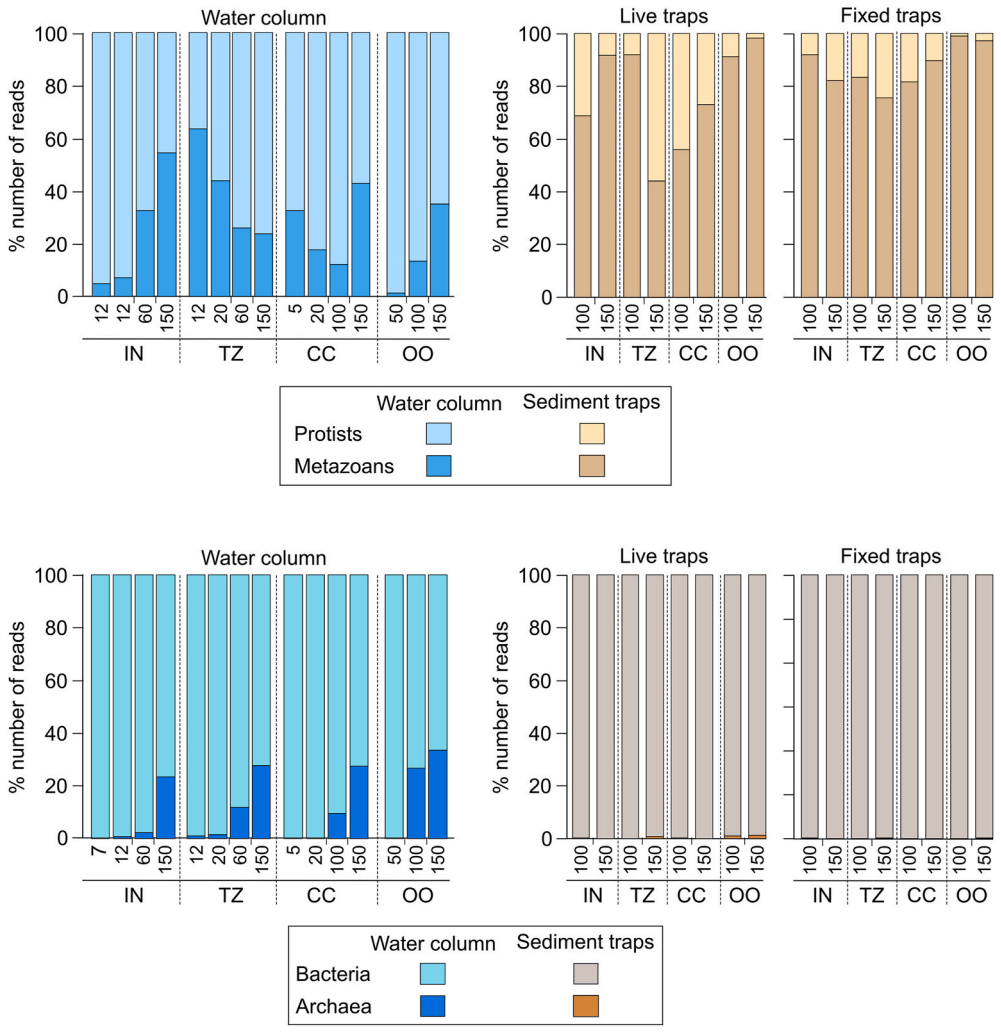

Fig. 3. Number of sequence reads of eukaryotes (18S rRNA, top panel) and prokaryotes (16S rRNA, bottom panel) in water-column and sediment-trap samples across an environmental gradient in the California Current Ecosystem. IN: inshore, TZ: transition zone, CC: California Current, OO: oligotrophic offshore.

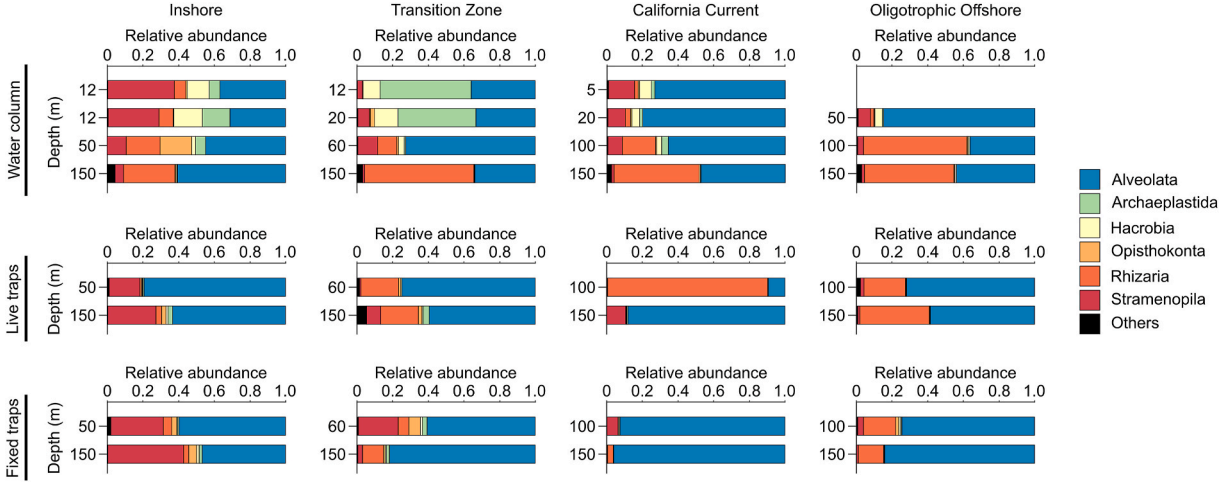

Fig. 4. Major groups of protists in the water column and sinking particles across an environmental gradient in the California Current Ecosystem, assessed by 18S V9 rRNA. Sinking particles were collected at two depths (base of the euphotic zone and 150 m) and trap tubes were filled with either a brine (live traps) or a RNA later solution (fixed traps).

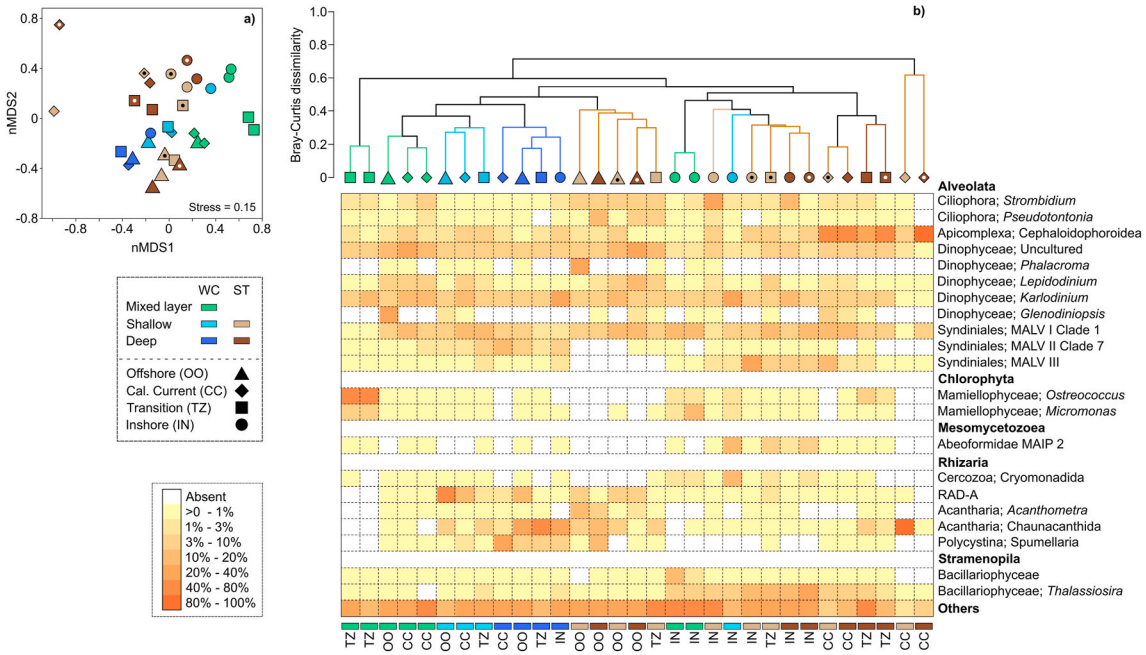

Fig. 5. Structure of the protist communities in the water column and sinking particles across an environmental gradient in the California Current Ecosystem. Non-metric multidimensional scaling (a) and dendrogram (b) based on the Bray-Curtis dissimilarity index. Colors indicate sample type (WC: water column, ST: sediment trap) and symbol shapes the sampling locations. Sinking particles in sediment traps were collected with either a brine (live traps) or a RNA later solution (fixed traps, symbols with a dot). Communities were grouped in thirteen significant clusters (SIMPROF, $p < 0.05$, black lines in cluster). Heatmap shows the relative abundances of the protists in each sample (i.e., each sample is 100%).

closely with sediment traps than other water-column samples, while the TZ mixed-layer assemblage is not similar to any other samples.

3.4. Sediment trap community composition: Eukaryotes

Alveolates and stramenopiles were all important in the IN traps, with high relative abundances of sequences assigned to the diatom *Thalassiosira* and syndiniales MALV III (Fig. 5b, Table S6). Alveolate sequences assigned to the apicomplexan Cephaloidophoroidea (likely parasitic protists) dominated protistan reads on sinking particles, especially at the TZ and CC sites (Fig. 5b). Alveolates and rhizarians were particularly important in OO samples. An uncultured dinoflagellate comprised ~10% of the total protistan sequence reads in this region, while the rhizarians included Chaunacanthida (class Acantharia) and Spumellaria (class Polycystina) (Fig. 5b). *Karlodinium*, an important dinoflagellate in water-column samples, contributed substantially to all trap samples (1–10% of reads), although it was only over-represented on sinking particles relative to water-column samples at the OO site (5–10% of reads) (Fig. 5b).

For sinking particles, the protist communities cluster mainly by site, with little difference between the base of the euphotic zone and 150 m depth (Fig. 5). OO samples form a distinct cluster with one of the shallow sediment traps from the TZ site. This cluster is more compositionally similar to water-column samples than to other trap samples, in part because apicomplexans comprise only a small component of the Alveolata in these samples (Fig. 5b). Trap sample sequences at the IN site (and one shallow TZ trap sample) cluster close to samples from the overlying mixed layer and the base of the euphotic zone at IN, all with high relative abundances of *Thalassiosira* (15–29% of reads). In contrast, CC and deep TZ trap samples with high contributions from apicomplexans (5–91% of reads) form distinct groups with low similarity to overlying water-column samples (Fig. 5b).

3.5. Major groups from sequence analyses: Prokaryotes

Bacteria sequences dominated water-column (92.6%) and trap (99.9%) 16S samples over Archaea (Fig. 3). In the mixed layer, Bacteroidetes and Proteobacteria dominate prokaryote sequences at the inshore sites (TZ and IN), and Proteobacteria and Cyanobacteria dominate at the offshore sites (OO and CC) (Fig. 6). Archaea, Bacteroidetes, and Proteobacteria are the main contributors at all sampling locations in the base of the euphotic zone and 150-m samples (Fig. 6). In contrast, sediment-trap sequences were mostly dominated by Proteobacteria at all sampling locations (Fig. 6), although relative abundances of Bacteroidetes are high in the IN, CC, and OO samples from the brine-filled traps, in conjunction with Cyanobacteria at the offshore sites (Fig. 6).

3.6. Water-column community composition: Prokaryotes

Similar to protists, the prokaryote assemblages show clear differences with depth (Fig. 7, Table S7). The mixed-layer communities have high relative abundances of cyanobacteria (*Prochlorococcus* and *Synechococcus)* and Alphaproteobacteria (SAR11 surface clade), with these three groups comprising 38% and 52% of the 16S rRNA gene sequences, respectively, at the offshore sampling locations (OO and CC) (Fig. 7b). *Synechococcus* was the most represented group, comprising 16% of reads, at the TZ site, and *Roseobacter* was conspicuously abundant at the IN site. Flavobacteria (multiple groups) were also proportionally more important at the TZ and IN sites (Fig. 7b).

At the base of the euphotic zone, Flavobacteria were fairly consistent contributors to prokaryotic sequences. The SAR11 surface clade was also important in CC and TZ waters. Archaea (Thaumarchaeota) increased substantially with depth (Fig. 7b). Bacteroidetes and Alphaproteobacteria were the main contributors in samples from the base of the euphotic zone and 150 m at all locations (Fig. 7b). SAR11 surface clade was also important at 150 m at all sites (Fig. 7b).

Bray-Curtis dissimilarity analysis shows a clear distinction between water-column (which cluster in one large group with ~50% similarity) and sediment trap samples (Fig. 7b). Within the water-column super group, 150-m samples comprise a distinct group with >80% similarity, identified by high proportional abundances of Thaumarchaeota and SAR11. This group is most closely associated with TZ, CC, and OO

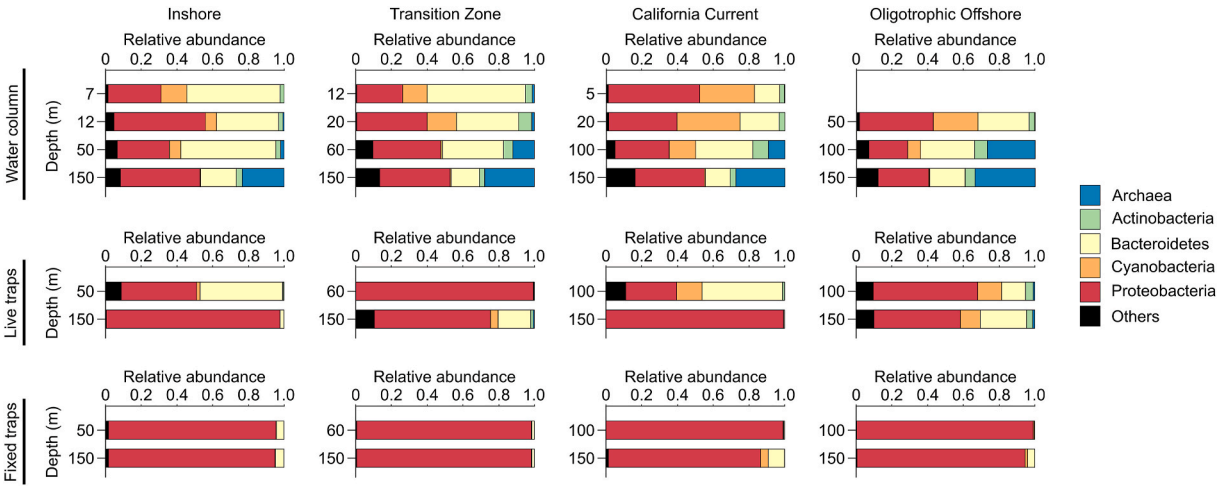

Fig. 6. Major groups of prokaryotes in the water column and sinking particles across an environmental gradient in the California Current Ecosystem, assessed by 16S rRNA. Sinking particles were collected at two depths (base of the euphotic zone and 150 m) and trap tubes were filled with either a brine (live traps) or a RNA later solution (fixed traps).

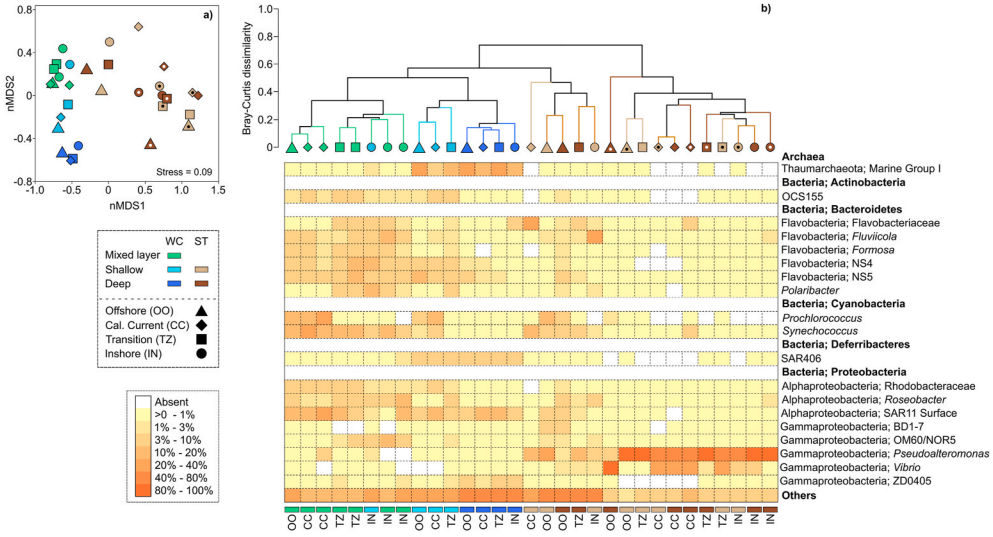

Fig. 7. Structure of the prokaryotic communities in the water column and sinking particles across an environmental gradient in the California Current Ecosystem. Non-metric multidimensional scaling (a) and dendrogram (b) based on the Bray-Curtis dissimilarity index. Colors indicate sample type (WC: water column, ST: sediment trap) and symbol shapes the sampling locations. Sinking particles in sediment traps were collected with either a brine (live traps) or a RNA later solution (fixed traps, symbols with a dot). Communities were grouped in twenty significant clusters (SIMPROF, $p < 0.05$, black lines in cluster). Heatmap shows the relative abundances of the prokaryotes in each sample (i.e., each sample is 100%).

samples from the base of euphotic zone, which have lower proportions of Thaumarchaeota and SAR11 and a greater influence of Flavobacteria. Mixed-layer samples fall into two subgroups based on relative system productivity, with TZ and IN samples separate from OO and CC samples (Fig. 7b).

3.7. Sediment trap community composition: Prokaryotes

Prokaryotic communities were distinctly different in trap samples compared to the water column (Fig. 7, Table S7). Gammaproteobacteria (*Pseudoalteromonas* and *Vibrio*) comprised the majority of reads at all locations (Figs. 6 and 7, Table S7), whereas variability in other groups drive cross-site differences. Unlike water-column or eukaryotic samples; however, there is not a clear pattern. Relative abundances of Bacteroidetes, Alphaproteobacteria, and Cyanobacteria were high in OO and CC samples from the brine-filled traps (Fig. 7b). *Prochlorococcus* and Gammaproteobacteria clade BD1-7 were major components of two OO samples, while the Flavobacteria *Fluviicola* was important in one IN sample (Fig. 7b). These relatively minor differences determined the clustering of samples in the dissimilarity analysis. However, the dissimilarity analysis did not elucidate clear patterns in the data, with most groups including samples from multiple sites and multiple depths. Across all sites, the general similarity and over-representation of Gammaproteobacteria on sinking particles is clear, in striking contrast to water-column assemblages and the variability of protistan communities on sinking particles.

3.8. Plastid sequences in sinking particles

Relative abundances of 16S and 18S rRNA gene sequences do not allow direct comparison of relative abundances of prokaryotes and eukaryotes. Hence, we analyzed plastid sequences to compare cyanobacteria and eukaryotic phytoplankton. Eighteen eukaryotic phytoplankton taxa were obtained from 16S rRNA gene sequencing of the water column and trap samples, with Mamiellophyceae, Prymnesiophyceae, and Bacillariophyceae exhibiting the greatest relative abundances in mixed-layer samples at the IN site (Fig. 8, Table S8). At this site, Bacillariophyceae was the only group that was over-represented in sediment traps (35% of plastid sequences) relative to the mixed layer (12.0%). Also, at the IN site, the relative abundances of Mamiellophyceae and Prymnesiophyceae were similar in traps and the water column, while cyanobacteria (*Synechococcus* and *Prochlorococcus*) were under-

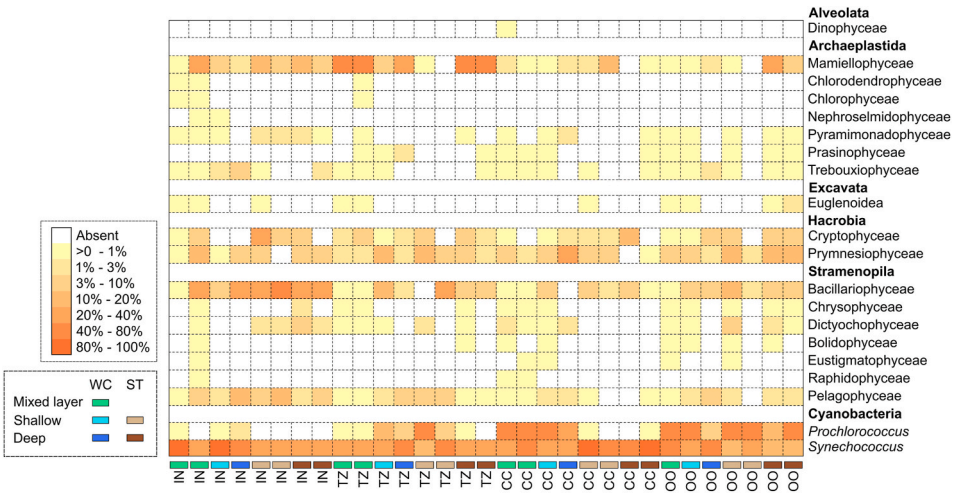

Fig. 8. Relative contribution of 16S plastid sequences in water column and sediment trap samples in the California Current Ecosystem. Colors indicate sample type (WC: water column, ST: sediment trap) (i.e., each sample is 100%).

represented in sinking particles relative to the water column. At the TZ site, mixed-layer plastid sequences were dominated by Mamiellophyceae (64.5%), which had lower proportional representation in shallow sediment traps, but roughly similar proportional representation in deep sediment traps (relative to the mixed layer). Meanwhile, *Synechococcus* (30.0% of plastid sequences at the TZ site) had a similar contribution to water column and the sediment traps. At the two offshore sites (CC and OO), the two cyanobacterial groups dominated the water-column plastid samples compared to eukaryotic phytoplankton, and *Synechococcus* was over-represented on sinking particles in the CC (but not OO) relative to the mixed layer, while *Prochlorococcus* was never over-represented on sinking particles. Across all sites, Bacillariophyceae proportions in the sediment trap samples were typically similar to or greater than its contribution to the mixed layer water column community (Fig. 8, Table S8).

4. Discussion

4.1. Environmental conditions during the 2015–2016 El Niño

The prolonged anomalous warm-water conditions that prevailed in the North Pacific from late 2013 to 2016 likely influenced the microbes contributing to sinking particles during our study. In the northern region of the California Current Ecosystem (CCE), considerable changes in the plankton communities (protists and zooplankton) were documented by Peterson et al. (2017), who found an increase in taxa with tropical-subtropical affinities, increased species richness of dinoflagellates, and reduced plankton biomass. During our study in the southern CCE, plankton with subtropical affinities were also evident (e.g., *Doliolum denticulatum*). However, the inshore-offshore distributions of the major groups of microbes were generally consistent with their normal ranges in the region (Freibott et al., unpublished), despite warmer than normal conditions (McClatchie et al., 2016). For example, the higher relative abundances of *Prochlorococcus* at the offshore sites (OO and CC) and of *Synechococcus* at the CC and TZ sites are consistent with their inshore-offshore biomass distributions (Taylor and Landry, 2018). Likewise, among protists primarily present in the mixed layer (Fig. 5), the dominance of dinoflagellates offshore and the importance of both diatoms and dinoflagellates inshore (assuming that syndiniales are mostly within their hosts) agree with the inshore-offshore contributions of these groups to protistan abundance and biomass in the CCE (Taylor et al., 2015; Venrick, 2002). The high dominance of rhizarians deep in the water column is consistent with their increased importance to plankton biomass with depth (Biard et al., 2018). In addition, particulate organic carbon fluxes during this study at the OO, CC, and TZ sites were within the ranges previously documented in the CCE, whereas at the IN site, fluxes were actually higher than prior measurements (Stukel et al., 2015). Although the effects of the 2015–2016 El Niño on the specific microbes exported are uncertain due to the lack of a basis of comparison, they are likely representative of conditions in the region because our sampling was done when El Niño was in decline.

4.2. Microbial communities and sinking particle flux: Ecosystem variability

Foundational studies relating food webs and the biological pump have highlighted the importance of large, mineral-ballasted phytoplankton, metazoan fecal pellets, and aggregates in sinking particle flux (Michaels and Silver, 1988; Passow et al., 1994; Smayda, 1971). Additional studies have documented heterogeneity of sinking particles and aggregates, including variability in the taxonomic composition and size of sinking particles (Durkin et al., 2015; Fender et al., 2019; McDonnell and Buesseler, 2010; Richardson, 2019), though without substantially changing the expectation for higher export efficiency in diatom- and mesozooplankton-dominated regions (Steinberg and Landry, 2017; Turner, 2015). Until recently, however, such studies have been severely limited by the poor taxonomic resolution of microscopy and pigment-based approaches to investigating microbial communities.

Next generation sequencing techniques now allow more detailed interrogation of microbial communities on sinking particles and in the mesopelagic realm generally (Amacher et al., 2009; Swan et al., 2011). These sequencing techniques have identified unexpected taxa that either correlate with export flux or are commonly associated with sinking material, including rhizarians, parasitic Syndiniales, and Flavobacteria (Boeuf et al., 2019; Fontanez et al., 2015; Guidi et al., 2016; Gutierrez-Rodriguez et al., 2019). Such studies have additionally raised new questions. For instance, Boeuf et al. (2019) found specialized piezophilic communities living on sinking particles in the bathypelagic, suggesting community evolution on sinking particles. In contrast, Mestre et al. (2018) observed similarities in microbial communities associated with large particles collected in surface, mesopelagic, and bathypelagic waters suggesting strong vertical connectivity. Sequencing has also given differing results with respect to the relative importance of cyanobacteria and eukaryotic phytoplankton (especially diatoms) on sinking material. Amacher et al. (2013) found that *Synechococcus* was often over-represented on sinking material in the Sargasso Sea relative to other cyanobacteria and eukaryotic plastids, and only rarely found genetic evidence of diatom plastids. In contrast, Preston et al. (2019)

analyzed sequences from a deep-sea time-series sediment trap in the northeast Pacific and found that a single diatom species (*Thalassiosira aestivalis*) accounted for 64% of all 18S rRNA gene sequences during the only high flux event in their dataset.

By sampling across an environmental gradient while simultaneously assessing suspended and sinking prokaryotic and eukaryotic communities, we are able to elucidate broad patterns in sinking microbial communities and reconcile some of these disparate results. We hypothesized that variability in the relative contributions of eukaryotic phytoplankton and microbial communities assessed in previous studies would be driven by variability in trophic structure. Specifically, we hypothesized that in productive ecosystems diatoms and rapidly sinking fecal pellets would promote vertical connectivity and hence greater similarity between euphotic zone microbial communities and microbial communities on sinking particles below the euphotic zone. In contrast, slower sinking rates and high recycling in oligotrophic regions would promote community succession on sinking particles, leading to communities on sinking particles that are largely distinct from the mixed layer. These relationships and mechanisms are generally supported by our results.

At the high-productivity, upwelling-influenced IN site, surface Chl *a* was 40 times higher than at the oligotrophic (OO) site and vertically-integrated primary production was nearly an order of magnitude higher (Figs. 1 and 2). This high productivity was associated with substantially higher export and a diatom-dominated phytoplankton community that was over-represented in sinking particles (Fig. 4). The IN site was also the only site for which Bray-Curtis dissimilarity analysis of protistan communities showed sediment trap and mixed layer communities clustering together (Fig. 5). For the remaining three sites, water-column communities clustered by depth, and sediment traps samples clustered separately. Particle-associated microbes at the richer upwelling IN site had high relative abundances of dinoflagellates (syndiniales MALV I, MALV III, and *Karlodinium*) and, notably, diatoms (an unclassified Bacillariophyceae and *Thalassiosira*). Microscopical analysis indicate that *Thalassiosira* cells are numerically important in mesotrophic CCE waters (Du et al., 2015), and that diatoms in general often dominate biomass in the coastal upwelling region (Taylor and Landry, 2018; Taylor et al., 2015). Although two diatom taxa were important in the water-column community at the IN site (Fig. 5), only *Thalassiosira* was strongly represented in the sediment trap material, likely transported to depth within copepod fecal pellets. Notably, this diatom species, responsible for 24% of protistan sequences in the deepest trap at the IN site, was closely related to the diatom that contributed 64% of all 18S rRNA gene sequences during the only high flux event sampled by Preston et al. (2019) in the bathypelagic. Overall, the strong similarity between euphotic zone and trap particle communities at the mesotrophic IN site suggests efficient export of "fresh" carbon from the ocean's surface, consistent with higher export expected for diatom-rich waters.

In stark contrast to our results at the IN site, the CC and OO sites showed strong dissimilarity between sediment trap and water-column communities (Fig. 5). Water-column communities clustered by depth, while the trap communities formed separate and distinct clusters. The protists on sinking particles at the OO site were characterized by high relative abundances of alveolates (mostly dinoflagellates) and rhizarians, consistent with their recognized importance on sinking particles (Amacher et al., 2009, 2013; Fontanez et al., 2015) and carbon export in oligotrophic systems (Guidi et al., 2016; Gutierrez-Rodriguez et al., 2019; Lampitt et al., 2009). Likewise, these groups are major components of protistan biomass in oligotrophic waters of the CCE (Biard et al., 2018; Taylor et al., 2015). Notably, the sinking material analyzed by microscopy at the OO site was mostly comprised of unrecognizable particles and aggregates, with very low pigment content (Fig. 2c–g). There were very few recognizable fecal pellets, although metazoans were actually a higher proportion of total reads than at other sites. Taken together, this suggests that sinking material in offshore oligotrophic waters is likely derived from fecal material, but aged and degraded during sinking, allowing substantial microbial colonization and community evolution. We also note that, although the coastal area was dominated by epipelagic taxa (e.g., diatoms) that contributed to export, export efficiency (i.e., carbon export/NPP) was not elevated in this region relative to offshore areas. This discrepancy likely arises from spatiotemporal decoupling of production and export, which has been described for the CCE region (Plattner et al., 2005; Kelly et al., 2018; Kahru et al., 2020), and leads to a supplement of organic matter input to offshore regions (Stephens *et al.* 2018). This organic matter subsidy increases export efficiency in the offshore regions relative to what would be expected in a one-dimensional system with oligotrophic communities. Disentangling these processes to quantify the relationship between epipelagic communities and export efficiency will require further sampling in coordination with mechanistic models.

The protists on sinking particles in the CC and TZ were dominated by the apicomplexan Cephaloidophoroidea and/or the acantharian Chaunacanthida. Acantharians are known for reproductive strategies that involve forming cysts, which sink rapidly due to their dense mineral (strontium sulfate) composition (Bernstein et al., 1987; Martin et al., 2010; Decelle et al., 2013). Because Chaunacanthida were important in the deeper water column at 150 m except at the CC, the high relative abundances of Chaunacanthida sequences in traps at this site could also reflect cyst sinking. We observed round structures similar to acantharian cysts in trap samples in the CC; however, these were considerably smaller (22–28 μm) than cysts collected in traps in the North Pacific (80–165 μm, Bernstein et al., 1987) and North Atlantic (200–1000 μm, Martin et al., 2010; Decelle et al., 2013). Cephaloidophoroidea is a poorly known group of gregarine apicomplexans that parasitize the intestines of crustaceans, including copepods (Rueckert *et al.*, 2011). The high relative abundances of apicomplexans in CC and TZ trap-collected particles coincide with the bloom of *D. denticulatum*. Due to the preferred particle sizes filtered by these doliolids (2.5–15 μm, Katechakis et al., 2004), it is unlikely that the parasites were acquired by feeding directly on copepods. Considering that other gregarine apicomplexans have been identified in guts of salps (Clopton, 2002; Wallis et al., 2017), Cephaloidophoroidea possibly also parasitize doliolids. Because doliolids are passive filter-feeders, the proportions of appropriately sized microbes in their diet should be similar to those in the water column (Alldredge and Madin, 1982). Nonetheless, at the sites where doliolids were most abundant, microbial communities in the water column and on sinking particles showed little similarity, suggesting substantial post-consumption transformations before particles were exported. The most notable contrast in the TZ was the virtual absence of *Ostreococcus*, a dominant mixed-layer picophytoplankton, on the sinking particles. *Ostreococcus* and *Micromonas* are both important components of the water-column communities in nutrient-rich regions of the CCE (Allen et al., 2012). It is possible, however, that the very tiny cells of *Ostreococcus* (~1 μm) were not efficiently grazed by *D. denticulatum* or rapidly degraded in the doliolid guts. In contrast to *Ostreococcus,* the relative abundances of two dinoflagellates (an uncultured taxon and *Karlodinium*) with lower contributions to the water-column assemblages were higher on sinking particles. These dinoflagellates were likely grazed and transported in doliolid fecal pellets.

4.3. Prokaryotic and eukaryotic communities associated with sinking particles

The above discussion highlights the impact of ecosystem trophic structure and food webs on the connectivity between water column and sinking microbial communities. However, many studies have found distinct microbial taxa, such as *Vibrio* and *Arcobacter*, associated with sinking particles (Boeuf et al., 2019; Guidi et al., 2016; Pelve et al., 2017). We hypothesize that eukaryotic organisms associated with sinking particles show greater compositional similarity to water-column communities than prokaryotic taxa, because they are more likely to sink individually, or within aggregates or fecal pellets. This hypothesis is

supported by our Bray-Curtis dissimilarity results showing that some protistan water-column communities cluster with trap-collected communities and vice versa (Fig. 5), while all prokaryotic water-column communities clustered within a single large group (Fig. 7).

These results agree with previous metabarcoding analyses from oligotrophic and mesotrophic systems that have shown significant differences in the community structure of water-column and trap-collected prokaryotes (Amacher et al., 2013; Fontanez et al., 2015; LeCleir et al., 2014). Among heterotrophic bacteria, mixed-layer sequences were mainly represented by members of Flavobacteria (NS4 and NS5 clades, *Fluviicola*) and Alphaproteobacteria (SAR11, *Roseobacter*), some of which are important free-living (e.g., SAR11) or particle-associated microbes in pelagic ecosystems (e.g., *Fluviicola, Roseobacter*) (DeLong et al., 1993). SAR11 relative abundances tended to be higher offshore (OO and CC) and were rarely major components of sinking particles. Allen et al. (2012) also documented that SAR11 sequences were rarely found in the largest size-fractions analyzed (3.0–200 μm). Likewise, the higher relative abundances of *Roseobacter* in nutrient-rich waters is consistent with Allen *et al.*'s (2012) findings in the CCE. Although *Roseobacter* are recognized as important colonizers of sinking particles (LeCleir et al., 2014), their relative abundances at the mesotrophic inshore sites (TZ and IN) during our study were similar in the water column and sinking particles. Also at the IN site, *Fluviicola* was the only heterotrophic bacterium significantly enriched on sinking particles, likely reflecting growth of these particle-associated bacteria during sinking (Suzuki et al., 2017). The increased importance of Archaea with depth at all sites is consistent with their vertical distribution (Karner et al., 2001) and their general absence on sinking particles collected in traps (Fontanez et al., 2015). In contrast, the dominance of *Pseudoalteromonas* and *Vibrio* (Gammaproteobacteria) sequences in trap-collected samples is consistent with their association with sinking particles or eukaryote surfaces and their enzymatic capabilities for degrading high molecular weight compounds (DeLong et al., 1993; Fontanez et al., 2015). *Pseudoalteromonas* are also known to produce anti-bacterial compounds (Holmström and Kjelleberg, 1999), which may allow them to dominate on particles by inhibiting the growth of other bacteria. In contrast, we suspect that *Synechococcus*, which was enriched on sinking particles only in oligotrophic regions, is often found in sediment trap results not because its ecology enhances carbon export, but rather because digestion-resistance properties enable it to survive intact (and be recognized) on sinking particles (Johnson et al., 1982; Valencia et al., 2021).

Although protistan groups in sediment traps generally showed greater similarity to mixed-layer communities, syndiniales (MALV), Cephaloidophoroidea, and Rhizaria were specific taxa associated with sinking particles. The importance of syndiniales and Cephaloidophoroidea on sinking particles suggests that these parasites might be transported within their eukaryotic hosts (Guillou et al., 2008). Although the mechanisms are not well understood, syndiniales, among parasites generally, appear to play important roles in modulating export flux (e.g., Amacher et al., 2013; Guidi et al., 2016). Rhizaria, meanwhile, are surmised to be important contributors to sinking particles both because they often reside in the mesopelagic, and because their siliceous tests promote sinking (Biard et al., 2016, 2018; Gutierrez-Rodriguez et al., 2019). In Valencia et al. (2021), we consider specific properties of these prokaryotic and protistan communities that make them more likely to be detected on sinking particles. Here, however, we simply note that the greater influence of mixed-layer communities on protistan, rather than prokaryotic, sinking particle-attached communities helps explain the greater temporal variability in protistan communities collected in time-series sediment traps (Boeuf et al., 2019; Preston et al., 2019).

5. Conclusions

Metabarcoding analyses of water-column and sediment trap samples from the CCE confirm some general findings from other systems, such as the strong associations of Gammaproteobacteria and rhizarians with particle export. Additionally, they provide new perspectives on variability within taxa and across gradients of ecosystem trophic state. For the former, we document differential sequence retention of *Thalassiosira* relative to co-occurring diatoms in sinking particles. We also find that protistan communities associated with sinking particles more closely resemble mixed-layer communities than prokaryotic communities on the same particles. Comparison of sites across an environmental gradient show that sinking particles beneath high-biomass, coastal upwelling-influenced water more closely resembles the water-column dominants (especially diatoms) found above, while oligotrophic communities exhibit greater dissimilarity between the microbial communities on sinking particles and in the mixed layer. These differences highlight important variability in microbial contributions to export from the water column between inshore mesotrophic and offshore oligotrophic waters that seem to align with differences in dominant grazing pathways (large copepods versus doliolids versus protistan microzooplankton) and export delivery mechanisms (fecal pellets versus aged amorphous aggregates).

Declaration of competing interest

The authors declare that they have no known competing financial interests or personal relationships that could have appeared to influence the work reported in this paper.

Acknowledgments

We thank the captain and crew of the R/V Sikuliaq for their help at sea. We also thank Mark Ohman for his leadership as Chief Scientist, Ralf Goericke, Megan Roadman, Tom Kelly, and all the scientists that participated on the CCE-LTER P1604 cruise, whose support made this study possible. We especially acknowledge Ali Freibott and Maitreyi Nagarkar for help with sample collection, processing, and bioinformatic analyses. We thank Hong Zheng for help with processing the molecular samples. This study was funded by the National Science Foundation grant OCE-1614359 to the CCE-LTER site. Analyses of molecular samples was partly funded by the Graduate Student Excellence Research Award of the Scripps Institution of Oceanography to B. Valencia. The Ph. D. research of B. Valencia was supported by a scholarship (529–2011) from the Colombian Administrative Department of Science, Technology and Innovation (COLCIENCIAS).

Appendix A. Supplementary data

Supplementary data to this article can be found online at https://doi.org/10.1016/j.dsr.2021.103668.

References

Alldredge, A.L., Madin, L.P., 1982. Pelagic tunicates: unique herbivores in the marine plankton. BioScience 32, 655–663.
Allen, L.Z., Allen, E.E., Badger, J.H., McCrow, J.P., Paulsen, I.T., Elbourne, L.D., Thiagarajan, M., Rusch, D.B., Nealson, K.H., Williamson, S.J., 2012. Influence of nutrients and currents on the genomic composition of microbes across an upwelling mosaic. ISME J. 6 (7), 1403–1414.
Amacher, J., Neuer, S., Anderson, I., Massana, R., 2009. Molecular approach to determine contributions of the protist community to particle flux. Deep-Sea Res. I 56 (12), 2206–2215.
Amacher, J., Neuer, S., Lomas, M., 2013. DNA-based molecular fingerprinting of eukaryotic protists and cyanobacteria contributing to sinking particle flux at the Bermuda Atlantic time-series study. Deep-Sea Research II 93, 71–83.
Amaral-Zettler, L.A., McCliment, E.A., Ducklow, H.W., Huse, S.M., 2009. A method for studying protistan diversity using massively parallel sequencing of V9 hypervariable regions of small-subunit ribosomal RNA genes. PLoS One 4 (7), e6372.
Bernstein, R.E., Betzer, P.R., Feely, R.A., Byrne, R.H., Lamb, M.F., Michaels, A.F., 1987. Acantharian fluxes and strontium to chlorinity ratios in the North Pacific Ocean. Science 237, 1490–1495.
Biard, T., Krause, J.W., Stukel, M.R., Ohman, M.D., 2018. The significance of giant phaeodarians (Rhizaria) to biogenic silica export in the California current ecosystem. Global Biogeochem. Cycles 32 (6), 987–1004.

Biard, T., Stemmann, L., Picheral, M., Mayot, N., Vandromme, P., Hauss, H., Gorsky, G., Guidi, L., Kiko, R., Not, F., 2016. In situ imaging reveals the biomass of giant protists in the global ocean. Nature 532 (7600), 504–507.
Boeuf, D., Edwards, B.R., Eppley, J.M., Hu, S.K., Poff, K.E., Romano, A.E., Caron, D.A., Karl, D.M., DeLong, E.F., 2019. Biological composition and microbial dynamics of sinking particulate organic matter at abyssal depths in the oligotrophic open ocean. Proc. Natl. Acad. Sci. Unit. States Am. 116 (24), 11824–11832.
Bond, N.A., Cronin, M.F., Freeland, H., Mantua, N., 2015. Causes and impacts of the 2014 warm anomaly in the NE Pacific. Geophys. Res. Lett. 42 (9), 3414–3420.
Buesseler, K.O., Boyd, P.W., 2009. Shedding light on processes that control particle export and flux attenuation in the twilight zone of the open ocean. Limnol. Oceanogr. 54 (4), 1210–1232.
Burd, A., Buchan, A., Church, M., Landry, M., McDonnell, A., Passow, U., Steinberg, D., Benway, H., 2016. In: Towards a Transformative Understanding of the Ocean's Biological Pump: Priorities for Future Research. Report of the NSF Biology of the Biological Pump Workshop, Feb. 19-20, 2016. Hyatt Place New Orleans, New Orleans, LA, p. 36.
Clopton, R.E., 2002. Phylum Apicoplexa Levine 1970: Order Eugregarinorida Léger, 1990. In: Lee, J.J., Leedale, G.F., Bradbury, P. (Eds.), Illustrated guide to the protozoa, 2nd edn. Society of Protozoologists, Lawrence, pp. 205–288.
Cram, J.A., Weber, T., Leung, S.W., McDonnell, A.M.P., Liang, J.-H., Deutsch, C., 2018. The role of particle size, ballast, temperature, and oxygen in the sinking flux to the deep sea. Global Biogeochem. Cycles 32 (5), 858–876.
Decelle, J., Martin, P., Paborstava, K., Pond, D.W., Tarling, G., Mahé, F., et al., 2013. Diversity, ecology and biogeochemistry of cyst-forming Acantharia (Radiolaria) in the oceans. PLoS One 8 (1), e53598.
DeLong, E.F., Franks, D.G., Alldredge, A.L., 1993. Phylogenetic diversity of aggregate-attached vs. free-living marine bacterial assemblages. Limnol. Oceanogr. 38 (5), 924–934.
Du, X., Peterson, W., O'Higgins, L., 2015. Interannual variations in phytoplankton community structure in the northern California Current during the upwelling seasons of 2001-2010. Mar. Ecol. Prog. Ser. 519, 75–87.
Ducklow, H.W., Steinberg, D.K., Buesseler, K.O., 2001. Upper ocean carbon export and the biological pump. Oceanography 14 (4), 50–58.
Durkin, C.A., Estapa, M.L., Buesseler, K.O., 2015. Observations of carbon export by small sinking particles in the upper mesopelagic. Mar. Chem. 175, 72–81.
Fender, C.K., Kelly, T.B., Guidi, L., Ohman, M.D., Smith, M.C., Stukel, M.R., 2019. Investigating particle size-flux relationships and the biological pump across a range of plankton ecosystem states from coastal to oligotrophic. Frontiers in Marine Science 6, 603.
Fontanez, K.M., Eppley, J.M., Samo, T.J., Karl, D.M., DeLong, E.F., 2015. Microbial community structure and function on sinking particles in the North Pacific Subtropical Gyre. Front. Microbiol. 6.
Frischknecht, M., Münnich, M., Gruber, N., 2018. Origin, transformation, and fate: the three-dimensional biological pump in the California current system. J. Geophys. Res.: Oceans 123 (11), 7939–7962.
Gong, W., Marchetti, A., 2019. Estimation of 18S gene copy number in marine eukaryotic plankton using a next-generation sequencing approach. Frontiers in Marine Science 6, 219.
Guidi, L., Chaffron, S., Bittner, L., Eveillard, D., Larhlimi, A., Roux, S., Darzi, Y., Audic, S., Berline, L., Brum, J.R., Coelho, L.P., Espinoza, J.C.I., Malviya, S., Sunagawa, S., Dimier, C., Kandels-Lewis, S., Picheral, M., Poulain, J., Searson, S., Tara Oceans Consortium, C., Stemmann, L., Not, F., Hingamp, P., Speich, S., Follows, M., Karp-Boss, L., Boss, E., Ogata, H., Pesant, S., Weissenbach, J., Wincker, P., Acinas, S.G., Bork, P., de Vargas, C., Iudicone, D., Sullivan, M.B., Raes, J., Karsenti, E., Bowler, C., Gorsky, G., 2016. Plankton networks driving carbon export in the oligotrophic ocean. Nature 532 (7600), 465–470.
Guillou, L., Viprey, M., Chambouvet, A., Welsh, R.M., Kirkham, A.R., Massana, R., et al., 2008. Widespread occurrence and genetic diversity of marine parasitoids belonging to Syndiniales (Alveolata). Environ. Microbiol. 10, 3349–3365.
Gutierrez-Rodriguez, A., Stukel, M.R., Lopes dos Santos, A., Biard, T., Scharek, R., Vaulot, D., Landry, M.R., Not, F., 2019. High contribution of Rhizaria (Radiolaria) to vertical export in the California Current Ecosystem revealed by DNA metabarcoding. ISME J. 13 (4), 964–976.
Holmström, C., Kjelleberg, S., 1999. Marine Pseudoalteromonas species are associated with higher organisms and produce biologically active extracellular agents. FEMS (Fed. Eur. Microbiol. Soc.) Microbiol. Ecol. 30 (4), 285–293.
Jackson, G.A., Najjar, R.G., Toggweiler, J.R., 1993. Flux feeding as a mechanism for zooplankton grazing and its implications for vertical particulate flux. Limnol. Oceanogr. 38 (6), 1328–1331.
Jacox, M.G., Hazen, E.L., Zaba, K.D., Rudnick, D.L., Edwards, C.A., Moore, A.M., Bograd, S.J., 2016. Impacts of the 2015–2016 El Niño on the California current system: early assessment and comparison to past events. Geophys. Res. Lett. 43 (13), 7072–7080.
Kahru, M., Jacox, M.G., Lee, Z., Kudela, R.M., Manzano-Sarabia, M., Mitchell, B.G., 2015. Optimized multi-satellite merger of primary production estimates in the California Current using inherent optical properties. J. Mar. Syst. 147, 94–102.
Kahru, M., Jacox, M.G., Ohman, M.D., 2018. CCE1: decrease in the frequency of oceanic fronts and surface chlorophyll concentration in the California Current System during the 2014–2016 northeast Pacific warm anomalies. Deep-Sea Res. I 140, 4–13.
Johnson, P.W., Huai-Shu, X., Sieburth, J.M., 1982. The utilization of chroococcoid cyanobacteria by marine protozooplankters but not by calanoid copepods. Ann. Inst. Oceanogr. Paris Nouv Ser 58, 297–308.
Kahru, M., Goericke, R., Kelly, T.B., Stukel, M.R., 2020. Satellite estimation of carbon export by sinking particles in the California Current calibrated with sediment trap data. Deep Sea-Research II 173, 104639.
Karner, M.B., DeLong, E.F., Karl, D.M., 2001. Archaeal dominance in the mesopelagic zone of the Pacific Ocean. Nature 409 (6819), 507–510.
Katechakis, A., Stibor, H., Sommer, U., Hansen, T., 2004. Feeding selectivities and food niche separation of Acartia clausi, Penilia avirostris (Crustacea) and Doliolum denticulatum (Thaliacea) in Blanes Bay (Catalan Sea, NW Mediterranean). J. Plankton Res. 26 (6), 589–603.
Kelly, T.B., Goericke, R., Kahru, M., Song, H., Stukel, M.R., 2018. CCE II: spatial and interannual variability in export efficiency and the biological pump in an eastern boundary current upwelling system with substantial lateral advection. Deep Sea Research I 140, 14–25.
Knauer, G.A., Martin, J.H., Bruland, K.W., 1979. Fluxes of particulate carbon, nitrogen, and phosphorus in the upper water column of the Northeast Pacific. Deep-Sea Res. 26 (1), 97–108.
Lampitt, R., Salter, I., Johns, D., 2009. Radiolaria: major exporters of organic carbon to the deep ocean. Global Biogeochem. Cycles 23 (1), GB1010.
Landry, M.R., Ohman, M.D., Goericke, R., Stukel, M.R., Tsyrklevich, K., 2009. Lagrangian studies of phytoplankton growth and grazing relationships in a coastal upwelling ecosystem off Southern California. Prog. Oceanogr. 83, 208–216.
LeCleir, G.R., DeBruyn, J.M., Maas, E.W., Boyd, P.W., Wilhelm, S.W., 2014. Temporal changes in particle-associated microbial communities after interception by nonlethal sediment traps. FEMS (Fed. Eur. Microbiol. Soc.) Microbiol. Ecol. 87 (1), 153–163.
Martin, P., Allen, J.T., Cooper, M.J., Johns, D.G., Lampitt, R.S., Sanders, R., Teagle, D.A., 2010. Sedimentation of acantharian cysts in the Iceland Basin: Strontium as a ballast for deep ocean particle flux, and implications for acantharian reproductive strategies. Limnol. Oceanogr. 55, 604–614.
Martin, J.H., Knauer, G.A., Karl, D.M., Broenkow, W.W., 1987. Vertex: carbon cycling in the northeast Pacific. Deep-Sea Res. 34 (2), 267–285.
McClatchie, S., Goericke, R., Leising, A., Auth, T., Bjorkstedt, E., Roberson, R.R., Brodeur, R.D., Du, X., Daly, E.A., Morgan, C.A., Chavez, F.P., Debich, A.J., Hildebrand, J., Field, J., Sakuma, K., Jacox, M., Kahru, M., Kudela, R., Anderson, C., Lavaniegos, B.E., Gomez-Valdes, J., Jimenez-Rosenberg, S.P.A., McCabe, R., Melin, S., Ohman, M.D., Sala, L.M., Peterson, B., Fisher, J., Schroeder, I.D., Bograd, S.J., Hazen, E.L., Schneider, S.R., Golightly, R.T., Suryan, R.M., Gladics, A. J., Loredo, S., Porquez, J.M., Thompson, A.R., Weber, E.D., Watson, W., Trainer, V., Warzybok, P., Bradley, R., Jahncke, M., 2016. State of the California current 2015–16: comparisons with the 1997–98 El Niño. California cooperative oceanic fisheries investigations. Data Rep. 57, 1–57.
McDonnell, A.M.P., Boyd, P.W., Buesseler, K.O., 2015. Effects of sinking velocities and microbial respiration rates on the attenuation of particulate carbon fluxes through the mesopelagic zone. Global Biogeochem. Cycles 29 (2), 175–193.
McDonnell, A.M.P., Buesseler, K.O., 2010. Variability in the average sinking velocity of marine particles. Limnol. Oceanogr. 55 (5), 2085–2096.
Mestre, M., Ruiz-González, C., Logares, R., Duarte, C.M., Gasol, J.M., Sala, M.M., 2018. Sinking particles promote vertical connectivity in the ocean microbiome. Proc. Natl. Acad. Sci. Unit. States Am. 115 (29), E6799–E6807.
Michaels, A.F., Silver, M.W., 1988. Primary production, sinking fluxes and the microbial food web. Deep-Sea Res. 35 (4), 473–490.
Morrow, R.M., Ohman, M.D., Goericke, R., Kelly, T.B., Stephens, B.M., Stukel, M.R., 2018. Primary productivity, mesozooplankton grazing, and the biological pump in the California current ecosystem: variability and response to El Niño. Deep-Sea Res. I 140, 52–62.
Nickels, C.F., Ohman, M.D., 2018. CCEIII: persistent functional relationships between copepod egg production rates and food concentration through anomalously warm conditions in the California Current Ecosystem. Deep-Sea Res. I 140, 26–35.
Ohman, M.D., Barbeau, K., Franks, P.J.S., Goericke, R., Landry, M.R., Miller, A.J., 2013. Ecological transitions in a coastal upwelling ecosystem. Oceanography 26 (3), 210–219.
Oksanen, J., Blanchet, F.G., Kindt, R., Legendre, P., Minchin, P., O'hara, R., Simpson, G., Solymos, P., Stevens, M., Wagner, H., 2017. Vegan: Community Ecology Package. R Package. Version.
Passow, U., Alldredge, A.L., Logan, B.E., 1994. The role of particulate carbohydrate exudates in the flocculation of diatom blooms. Deep-Sea Res. I 41 (2), 335–357.
Pelve, E.A., Fontanez, K.M., DeLong, E.F., 2017. Bacterial succession on sinking particles in the ocean's interior. Front. Microbiol. 8 (2269).
Peterson, W.T., Fisher, J.L., Strub, P.T., Du, X., Risien, C., Peterson, J., Shaw, C.T., 2017. The pelagic ecosystem in the Northern California Current off Oregon during the 2014–2016 warm anomalies within the context of the past 20 years. J. Geophys. Res.: Oceans 122 (9), 7267–7290.
Piontek, J., Handel, N., Langer, G., Wohlers, J., Riebesell, U., Engel, A., 2009. Effects of rising temperature on the formation and microbial degradation of marine diatom aggregates. Aquat. Microb. Ecol. 54 (3), 305–318.
Plattner, G.K., Gruber, N., Frenzel, H., McWilliams, J.C., 2005. Decoupling marine export production from new production. Geophys. Res. Lett. https://doi.org/10.1029/2005GL022660.
Preston, C.M., Durkin, C.A., Yamahara, K.M., 2019. DNA metabarcoding reveals organisms contributing to particulate matter flux to abyssal depths in the North East Pacific ocean. Deep-Sea Research II, 104708.
Quince, C., Lanzen, A., Davenport, R.J., Turnbaugh, P.J., 2011. Removing noise from pyrosequenced amplicons. BMC Bioinf. 12 (1), 1–18.
Richardson, T.L., 2019. Mechanisms and pathways of small-phytoplankton export from the surface ocean. Annual Review of Marine Science 11, 57–74.
Ruiz-González, C., Mestre, M., Estrada, M., Sebastián, M., Salazar, G., Agustí, S., Moreno-Ostos, E., Reche, I., Álvarez-Salgado, X.A., Morán, X.A.G., 2020. Major imprint of surface plankton on deep ocean prokaryotic structure and activity. Mol. Ecol. 29 (10), 1820–1838.

Siegel, D.A., Buesseler, K.O., Behrenfeld, M.J., Benitez-Nelson, C.R., Boss, E., Brzezinski, M.A., Burd, A., Carlson, C.A., D'Asaro, E.A., Doney, S.C., 2016. Prediction of the export and fate of global ocean net primary production: the EXPORTS science plan. Frontiers in Marine Science 3, 22.

Smayda, T.J., 1971. Normal and accelerated sinking of phytoplankton in sea. Mar. Geol. 11 (2), 105–122.

Steinberg, D.K., Landry, M.R., 2017. Zooplankton and the ocean carbon cycle. Annual Review of Marine Science 9, 413–444.

Stephens, B., Porrachia, M., Dovel, S., Roadman, M., Goericke, R., Aluwihare, L., 2018. Non-sinking organic matter production in the California Current. Global Biogeochem. Cycles 32 (9), 1386–1405.

Stukel, M.R., Barbeau, K.A., 2020. Investigating the nutrient landscape in a coastal upwelling region and its relationship to the biological carbon pump. Geophys. Res. Lett. 47 (6), e2020GL087351.

Stukel, M.R., Kahru, M., Benitez-Nelson, C.R., Decima, M., Goericke, R., Landry, M.R., Ohman, M.D., 2015. Using Lagrangian-based process studies to test satellite algorithms of vertical carbon flux in the eastern North Pacific Ocean. J. Geophys. Res.: Oceans 120, 7208–7222.

Stukel, M.R., Kelly, T.B., Aluwihare, L.I., Barbeau, K.A., Goericke, R., Krause, J.W., Landry, M.R., Ohman, M.D., 2019a. The Carbon:^{234}Thorium ratios of sinking particles in the California Current Ecosystem 1: relationships with plankton ecosystem dynamics. Mar. Chem. 212, 1–15.

Stukel, M.R., Ohman, M.D., Benitez-Nelson, C.R., Landry, M.R., 2013. Contributions of mesozooplankton to vertical carbon export in a coastal upwelling system. Mar. Ecol. Prog. Ser. 491, 47–65.

Stukel, M.R., Ohman, M.D., Kelly, T.B., Biard, T., 2019b. The roles of filter-feeding and flux-feeding zooplankton as gatekeepers of particle flux into the mesopelagic ocean. Frontiers in Marine Science 6, 397.

Suzuki, S., Kaneko, R., Kodama, T., Hashihama, F., Suwa, S., Tanita, I., Furuya, K., Hamasaki, K., 2017. Comparison of community structures between particle-associated and free-living prokaryotes in tropical and subtropical Pacific Ocean surface waters. J. Oceanogr. 73 (3), 383–395.

Swan, B.K., Martinez-Garcia, M., Preston, C.M., Sczyrba, A., Woyke, T., Lamy, D., Reinthaler, T., Poulton, N.J., Masland, E.D.P., Gomez, M.L., Sieracki, M.E., DeLong, E.F., Herndl, G.J., Stepanauskas, R., 2011. Potential for chemolithoautotrophy among ubiquitous bacteria lineages in the dark ocean. Science 333 (6047), 1296–1300.

Taylor, A.G., Landry, M.R., 2018. Phytoplankton biomass and size structure across trophic gradients in the southern California Current and adjacent ocean ecosystems. Mar. Ecol. Prog. Ser. 592, 1–17.

Taylor, A.G., Landry, M.R., Selph, K.E., Wokuluk, J.J., 2015. Temporal and spatial patterns of microbial community biomass and composition in the Southern California Current Ecosystem. Deep-Sea Research II 112, 117–128.

Turner, J.T., 2015. Zooplankton fecal pellets, marine snow, phytodetritus and the ocean's biological pump. Prog. Oceanogr. 130, 205–248.

Valencia, B., Stukel, M.R., Allen, A., McCrow, J.P., Rabines, A., Palenik, B., Landry, M.R., 2021. Relating sinking and suspended microbial communities in the California Current Ecosystem: digestion resistance and the contributions of phytoplankton taxa to export. Environ. Microbiol. https://doi.org/10.1111/1462-2920.15736.

Vandeputte, D., Kathagen, G., D'hoe, K., Vieira-Silva, S., Valles-Colomer, M., Sabino, J., Wang, J., Tito, R.Y., De Commer, L., Darzi, Y., 2017. Quantitative microbiome profiling links gut community variation to microbial load. Nature 551 (7681), 507–511.

Venrick, E.L., 2002. Floral patterns in the California current system off southern California: 1990-1996. J. Mar. Res. 60 (1), 171–189.

Wallis, J.R., Smith, A.J., Kawaguchi, S., 2017. Discovery of gregarine parasitism in some Southern Ocean krill (Euphausiacea) and the salp Salpa thompsoni. Polar Biol. 40, 1913–1917.

Whitaker, D., Christman, M., 2014. Clustsig: significant cluster analysis. R package version 1 (2), 4-2.